# Study of the Effects of the Prefilled-Plasma Parameters on the Operation of a Short-Conduction Plasma Opening Switch

Amit Weingarten, Vladimir A. Bernshtam, Amnon Fruchtman, Chris Grabowski, Yakov E. Krasik, and Yitzhak Maron

*Abstract*— **Spectroscopic methods are used to determine the density, the temperature, the composition, the injection velocity, and the azimuthal uniformity of the flashboard-produced prefilled plasma in an 85-ns, 200-kA plasma opening switch (POS). The electron density is found to be an order of magnitude higher than that obtained by charge collectors, which are commonly used to determine the density in such POS's, suggesting that the density in short conduction POS's is significantly higher than is usually assumed. We also find that the plasma is mainly composed of protons. The spectroscopically measured plasma parameters are used here to calculate the conduction currents at the time of the opening predicted by various theoretical models for the POS operation. Comparison of these calculated currents to the measured currents indicates that the plasma behavior during conduction is governed either by plasma pushing or by magnetic-field penetration and less by sheath widening near the cathode, as described by existing models. Also, the conduction current mainly depends on the prefilled electron density and less on the plasma flux, which is inconsistent with the predictions of the erosion (four-phase) model for the switch operation. Another finding is that a better azimuthal uniformity of the prefilled plasma density shortens the load-current rise time.**

*Index Terms*— **Plasma devices, plasma measurements, pulse power system switches.**

## I. Introduction

PLASMA opening switches (POS's) are used in pulsed power systems as intermediate stages between pulse generators and various loads [1]. The generator current flows through a prefilled plasma and energy is stored inductively until the POS opens rapidly and the current flows to a load. The use of a POS results in shortening of the load current rise time [2] as well as in power and voltage multiplication in inductive energy storage systems [3], and improved energy coupling to loads [4], [5]. POS's have been shown [6] to operate over both a wide range of currents times (from a few kA up to several MA) and conduction times (from 10's of ns to a few $\mu$s). Opening times can be as short as 10 ns for the short-conduction POS (ns POS), which conducts the current during $\leq$100 ns, and 50 ns for the long-conduction POS ($\mu$s- POS).

Several processes that may occur in the plasma during the current conduction were suggested to lead to the current interruption and switch opening. These are sheath widening near the cathode [2], [7]–[11], fast magnetic field penetration into the plasma [12], [13], pushing of the plasma by the magnetic field pressure [6], and development of plasma turbulence [14] that gives rise to anomalous resistivity. The relative dominance of these processes depend crucially on the plasma parameters [15]. Plasma erosion near the cathode, which is accompanied by the formation of a bipolar sheath and a vacuum gap, and can be described by the four-phase model [7], is expected to be the dominant mechanism in the POS opening at densities below $\approx 1 \times 10^{13}$ cm$^{-3}$. Other mechanisms that cause a sheath widening near the cathode may be dominant at higher densities [8]–[11]. Magnetic field penetration into the plasma due to the Hall field with a negligible ion motion, which is described by electron-magneto-hydrodynamic (EMHD) theory, is expected to limit the current conduction through the POS at densities up to a few times $10^{14}$ cm$^{-3}$. At higher densities, POS operation is predicted to be dominated by MHD pushing of the plasma [16] or by MHD pushing mixed with a Hall-field-induced magnetic field penetration [17]. In addition to the electron density, the dominance of each process also depends on the POS dimensions and geometry, on the plasma composition, on the voltage polarity, and on the injection velocity [15], [18].

The electron density in long conduction POS's was measured using He-Ne laser interferometry and was found to be between $4 \times 10^{14}$ cm$^{-3}$ and $2 \times 10^{16}$ cm$^{-3}$ [19]. The current conducted agreed well with the value expected when MHD pushing is dominant [16], [19]. During current conduction a significant plasma motion was observed [20], but magnetic field measurements [21] showed that there was a significant magnetic field penetration.

In the short-conduction POS, fast magnetic field penetration into the prefilled plasma region was observed [22] and explained by an EMHD theory [23]. Recently, we have shown [24] a quantitative agreement between the magnetic field evolution observed in a coaxial POS operating with a positive polarity of the inner electrode and the predictions of a two-dimensional EMHD model. In that experiment the plasma produced by a gas discharge was mainly composed of CIII and CIV, and its density was $(1 \pm 0.5) \times 10^{14}$ cm$^{-3}$.

Manuscript received June 10, 1999; revised September 16, 1999. This work was supported in part by the Minerva Foundation, Munich, Germany, and by the Israeli Academy of Science.

A. Weingarten, V. A. Bernshtam, C. Grabowski, and Y. Maron are with the Faculty of Physics, Weizmann Institute of Science, Rehovot 76100, Israel (e-mail: fnweing@plasma-gate.weizmann.ac.il).

A. Fruchtman is with the Sciences Department, Center for Technological Education Holon, Holon 58102, Israel.

Ya. E. Krasik is with the Physics Department, Technion—Israel Institute of Technology, Haifa 32000, Israel.

Publisher Item Identifier S 0093-3813(99)09857-4.

The density of the plasma in short conduction POS's, produced by flashboards or plasma guns [6], has usually been measured by electric probes and charge collectors [25], [26] and has been found to be between $1 \times 10^{12}$ cm$^{-3}$ and $1 \times 10^{14}$ cm$^{-3}$ [1]. As we mentioned above, at this low density regime, plasma erosion is expected to be dominant. Indeed, it was claimed [25], [26] that the current conducted by the POS agreed reasonably well with the predictions of the four-phase erosion model. In these estimates, it was assumed based on line-emission [26], [27] or the plasma source substrate [20] that the ions are CII and CIII.

In this paper we study the effects of the prefilled-plasma parameters on the maximal conduction current and on the conduction and opening times in a short conduction plasma opening switch. We present the results of electron density measurements that were performed using two independent spectroscopic techniques in a 200-kA, 85-ns POS experiment. First, the electron density of the flashboard-produced plasma in the POS region is determined as a function of time using Stark broadening of hydrogen lines. This technique yields the density integrated over the axial line of sight. In the second technique, a lower bound on the density is obtained from level-population ratios of MgII. The magnesium ions are introduced into the plasma by locally doping the prefilled plasma using laser evaporation [28]. This allows for doping the plasma with various ions whose spectral lines are suitable for the different measurements, and for obtaining measurements which are spatially resolved in the axial direction. The density of the plasma measured spectroscopically is found to range from $(7 \pm 2) \times 10^{13}$ cm$^{-3}$ to $(3 \pm 0.5) \times 10^{14}$ cm$^{-3}$, for conduction times ranging from 40 ns to 100 ns, respectively.

We also measure the electron density using electric probes which, as stated before, are commonly used to determine the density in ns POS's. These measurements yield a density which is much lower than that determined spectroscopically. For our plasma parameters electric probes may not be adequate since they become saturated. Thus, the density obtained from the two independent spectroscopic measurements, with the uncertainties given above, reflects the true electron density in the plasma. It is, therefore, possible that in those previous ns-POS experiments the density was actually much higher than was assumed.

We also measure in detail the plasma composition which is a highly important parameter in determining the POS conduction. It is shown here that in our flashboard-produced plasma, the most abundant ions in the plasma are protons. It is shown that near the cathode protons contribute $\approx$70% of the ionic charge, while closer to the anode the heavy ion fraction becomes larger, $\approx$ 75% of the ionic charge. We study the azimuthal uniformity of the electron density and found that a better azimuthal uniformity shortens the rise time of the load current.

In Section II, the POS, the plasma source, and the diagnostics are presented, and in Section III, the experimental results are described. In Section IV, we discuss the effects of the prefilled-plasma parameters on the POS operation. In particular, we examine the dependence of the POS maximal conduction current on the electron density and compare it to the theoretical models. We conclude that in a short conduction POS the plasma behavior during conduction seems to be governed either by plasma pushing or by magnetic field penetration and less by sheath widening near the cathode.

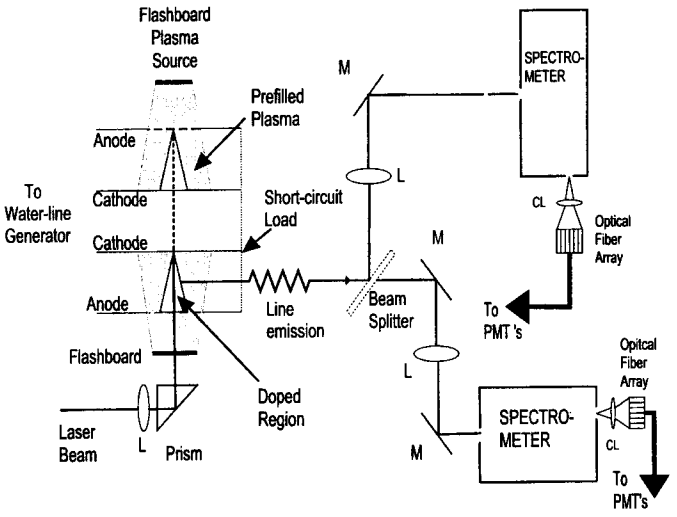


Fig. 1. POS system and the spectroscopic diagnostics. The prefilled plasma is produced by the flashboard and injected radially inward through the anode. The focused laser pulse is aligned to either of the POS electrodes, in order to evaporate material and achieve local measurements. The light emitted by the plasma and the doped ions is directed by a beam splitter onto the two spectrometers. The dispersed light is collected by photomultiplier tubes.

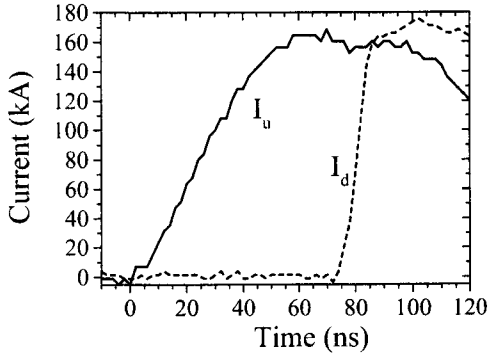


Fig. 2. Generator ($I_u$, solid line) and load ($I_d$, dashed line) currents.

## II. Experimental System and Diagnostics

The POS, shown schematically in Fig. 1, is coaxial with the inner electrode charged negatively. The inner and outer electrode diameters are 4 and 9 cm, respectively, and the plasma axial length (full width half maximum, FWHM) was varied in the experiment from 6 to 10 cm. The inductances of the transmission line upstream and downstream of the prefilled plasma are $L_U = 95$ nH and $L_D = 25$ nH, respectively. A 300-kV voltage pulse is applied to the inner electrode by a 4 kJ, 1 $\Omega$, $LC$-water-line Marx generator, producing a current pulse with a quarter period of 85 ns and a peak current of 200 kA (depending on the POS conduction duration due to the changes in the inductance). Typical generator (upstream) current and load (downstream) current, measured by calibrated Rogowski coils, are shown in Fig. 2.

Two 1-m spectrometers each equipped with a 2400 groove/mm grating giving a spectral resolution of 0.06 Å and a dispersion of 2–3 Å/mm are used for the spectroscopic observations. The diagnostic system, shown in Fig. 1, allows for axial line of sight over the entire POS gap. A few imaging systems that image a rectangular section of the plasma onto the spectrometers input slits are used. Mirrors are used to obtain measurements at different radial and azimuthal positions. The spatial resolution in the radial and azimuthal directions is 1–2 mm. The light from each spectrometer output slit is imaged by a cylindrical lens onto an optical fiber-bundle array (fiber diameter of 250 $\mu$m). The distance between each spectrometer output slit and the optical fiber-bundle, and the position of the cylindrical lens, are varied to change the magnification of the spectrometer dispersed light. This allows for choosing the spectral separation between the optical fibers suitable for the different measurements. The light is then transmitted by the optical fibers to a set of 10 photomultiplier tubes (PMT) that have a response time of 4 ns. The time-dependent spectral profile is recorded on multichannel digitizers. Absolute calibration of the diagnostic systems was performed.

Plasma doping is performed using a Nd:YAG laser pulse (<100 mJ, 10 ns FWHM) that evaporates materials deposited on either of the two POS electrodes [28]. For doping off the anode, the laser beam is passed between the cathode slots. The laser pulse forms a plasma column with $\approx$45° divergence angle that flows into the POS region. The doping column axial position is varied in the experiments by changing the position of the prism $P$ (see Fig. 1).

The plasma was also investigated using arrays of up to 11 negatively biased charge collectors (Faraday cups) that were spaced axially 1.2 cm apart. Up to four arrays can be used in a single shot, positioned at 90° with respect to one another. The arrays can be rotated in order to view the plasma injected at any azimuth and can also be axially and radially translated. The diameter of the collimating hole in each cup is 0.05 cm, allowing particles with a divergence angle of 45° to be collected. In addition, measurements were performed using a single Langmuir probe made of 1-cm long, 200-$\mu$m diameter tungsten wire.

The plasma source was designed for achieving versatility in the prefilled plasma parameters. The plasma is produced using two flashboard arrays, which are similar to the ones described in [29]. However, in order to achieve better control over the plasma parameters, each flashboard has been made of two boards: one on which the discharge gaps are printed and the other serving as the ground electrode that carries the return current. It was found that varying the spacing between these two boards affects the electron density and injection velocity. For this coaxial experiment, the flashboards are bent to form a cylinder located 6.5 cm outside the outer electrode. Several flashboard configurations, differing in the number and size of the discharge gaps, the number of chains, and the capacitance of the driving capacitor bank (0.22 $\mu$F $\leq C \leq$ 0.9 $\mu$F; 16 kV $\leq V \leq$ 35 kV) were tested. The flashboard discharge gaps are coated with graphite to enable operation at relatively low charging voltage of the driving capacitor bank. The plasma that is produced flows through the 85% transparency anode into the POS region.

## III. Measurements

### A. Density of the Prefilled Plasma

The time-dependent electron density ($n_e$) of the prefilled plasma is determined from $H_\alpha$ and $H_\beta$ Stark broadening. The experimental line widths are fitted self-consistently assuming that the lines are broadened by Stark and Doppler effects [30], [31]. A quasi-static approximation for the perturbing ions is used in the Stark calculations; i.e., we neglect the effect of the ion motion on the relevant time scale [30], [31] which is the inverse of the line half FWHM (on the order of few ps). For our plasma parameters, this approximation is well known to be valid for $H_\beta$. For $H_\alpha$ the Doppler dominates the broadening and the inclusion of the ion dynamics negligibly affect the results [32]. In the calculation, the Doppler contribution is assumed to be Gaussian. This assumption is found to give a satisfactory fit of the calculated to the observed line profiles. We note that in these calculations we assume that the perturbers are singly charged ions. The correction for the inclusion of the multiply charged ions is discussed in Section III-C. Since electric fields resulting from the flashboard current may affect the Stark broadening of the hydrogen lines we have taken measures to eliminate such fields by screening the fields using a thin grid of 90% transparency placed 3 cm from the flashboard surface.

The electron density for the flashboard configuration used in the POS experiments is shown in Fig. 3 for a few radial positions. For this flashboard configuration, optimal POS operation is achieved when the generator-current pulse is applied (2.3 $\pm$ 0.1) $\mu$s after the flashboard is discharged (we define the optimal POS operation when the POS reaches full opening at $t = 85 \pm 7$ ns, delivering the maximum current to the load). At this time, the electron density over the entire measured region is determined to be (2.4$\pm$0.4) $\times$ $10^{14}$ cm$^{-3}$. At each instant, the density is similar at all radii, although at each radial position it is increasing in time up to $t > 3$ $\mu$s. This indicates that the inward geometrical convergence of the flowing plasma approximately compensates for the increasing distance from the flashboard.

We have also performed plasma-density measurements using charge collectors and electric probes. At the time of interest, the charge collectors show a density that is by an order of magnitude lower than that obtained using spectroscopy. The time-dependent radial ion flux collected by the charge collectors when placed at $r = 3$ cm is shown in Fig. 4(a). Fig. 4(b) shows the density determined spectroscopically and the intensities of $H_\alpha$ and the CIII 2297-Å line. At the early times, no line emission is observed and the charge collectors most probably show the protons propagating ahead of the hydrogen-carbon plasma. The peak flux measured by the charge collectors, reached at $t = 1.9$ $\mu$s, is $4 \times 10^{19}$ cm$^{-2}$ s$^{-1}$. A lower limit for the ion radial velocity, estimated assuming the ions are formed at $t = 0$ at the flashboard at a distance $d$ from the charge collectors, is $v_{\min}(t) = \frac{d}{t} \simeq 4 \times 10^6$ cm/s.

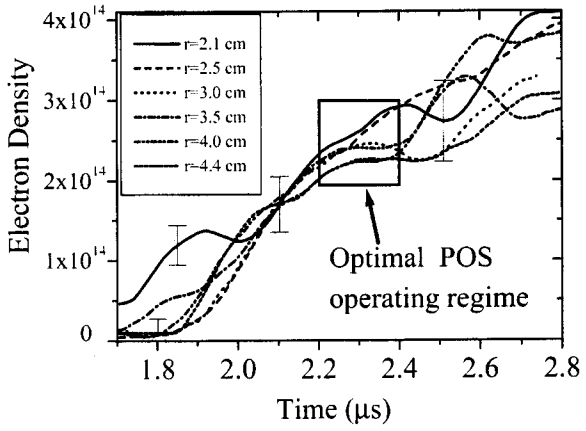


Fig. 3. Prefilled-plasma electron density as a function of time at a few radial positions obtained from Stark broadening of hydrogen lines. The density is averaged along the $z$ direction.

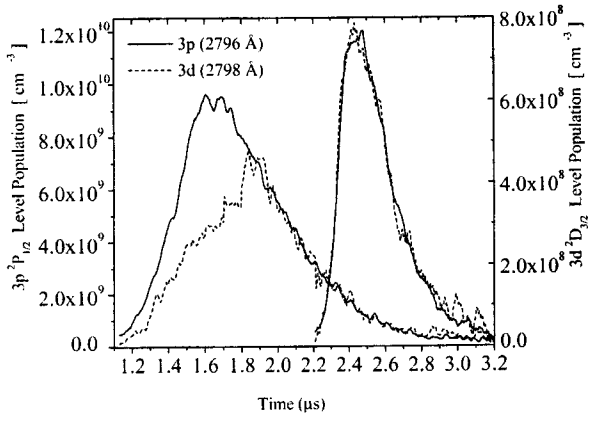


Fig. 5. Time dependent populations of the MgII 3p $^2P_{1/2}$ level ($E_{exc}$ = 4.4 eV, 2796 Å line) and the 3d $^2D_{3/2}$ level ($E_{exc}$ = 8.9 eV, 2798 Å line), observed by two spectrometers in the same discharge. Two discharges with different laser timings are shown.

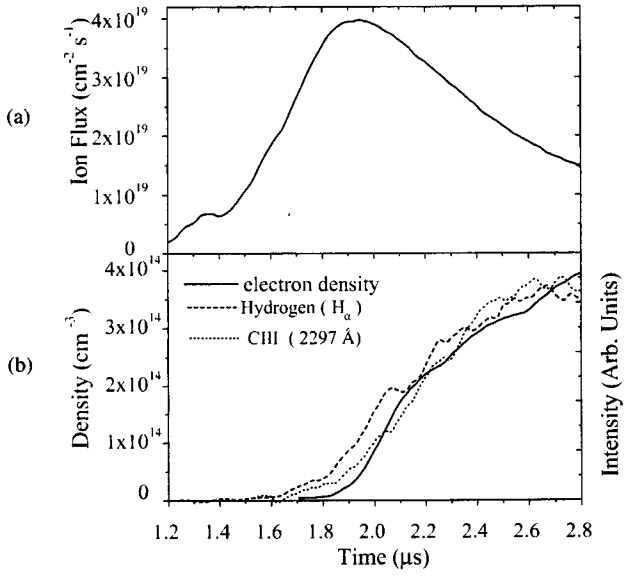


Fig. 4. (a) Plasma flux obtained from the charge-collector measurements. (b) The density obtained from Stark broadening of hydrogen lines (solid line), $H_\alpha$ (dashed line), and CIII line (dotted line) intensities (in arbitrary units). All the measurements are taken at $r$ = 3 cm. The comparison shows that the charge collectors are saturated already by the relatively-low-density proton plasma propagating ahead of the carbon ions.

Therefore, the maximum density determined from the charge collectors is $\simeq 1 \times 10^{13}$ cm$^{-3}$. At this time, the electron density obtained from the hydrogen lines (Fig. 3) is already 2–3 times higher. At later times, the ion flux decreases and the density obtained from the charge collectors does not increase, while the density obtained spectroscopically rises. The line intensities of the $H_\alpha$ and CIII show a temporal behavior similar to that of the electron density obtained spectroscopically.

We believe that at later times ($\geq 2$ μs) the charge collectors are saturated and not all the ions are collected. This probably occurs since the density inside the cup is too high, and because secondary plasma is produced at the collector entrance by the fast proton plasma. Measurements with a single Langmuir probe gave a temporal dependence similar to that of the charge collectors, since the ion directed velocity significantly exceeds the ion thermal velocity. The CIII radial directed velocity is determined by time-of-flight calculation from the carbon line emission to be $\simeq 6 \times 10^6$ cm/s, while the thermal velocity, determined from the Doppler width, is $< 2 \times 10^6$ cm/s. The proton temperature cannot be measured directly, but can be estimated from the temperature of the other ions to be $\leq 20$ eV, corresponding to a velocity of $\leq 4 \times 10^6$ cm/s. The proton directed velocity, determined by time-of-flight calculations from the charge collector signals, is $\geq 1 \times 10^7$ cm/s. Thus, the ion directed current is much larger than the probe ion-saturation current (the Bohm current), and the probes could not be used to determine the density. To conclude, the density obtained from electric-probe measurements has been found here to be lower than the true density by an order of magnitude, which is possible to occur in other POS experiments as well.

### *B. Electron Temperature and Density from MgII Line Ratio*

The electron density and temperature are also studied using the line intensities of MgII doped in the plasma and collisional radiative (CR) calculations [33]. Fig. 5 shows the time dependent populations of the MgII 3p $^2P_{1/2}$ level (excitation energy of 4.4 eV) and the 3d $^2D_{3/2}$ level (8.9 eV) at $r$ = 2.5 cm and $z$ = 0 cm obtained in two flashboard discharges. The two lines are observed simultaneously by the two spectrometers, and the timing of the evaporating laser pulse (relative to the flashboard discharge) is varied between the discharges. Knowledge of the density of the ions whose lines are measured and of the wavelength sensitivity of the spectroscopic system are not required, since the ratio of two lines of the same charge-state and of similar wavelength is used.

The population ratio of these two levels is sensitive to both the electron density and the electron temperature, since the 3d level can be either directly excited from the ground state (which requires electrons with energy $\geq 8.9$ eV) or by excitation from the 3p level (requiring two electron collisions but each with energy $\geq 4.4$ eV). For our plasma parameters (far from the local thermal equilibrium or corona limits), the excitation by a single collision causes the line ratio to be sensitive to the temperature. Excitation by two collisions

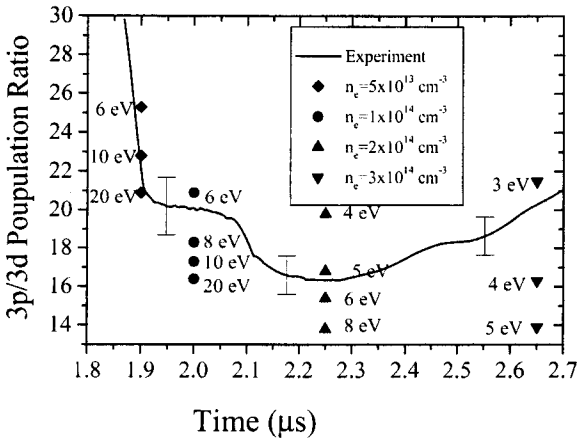


Fig. 6. Experimental population ratio of the MgII 3p $^2P_{3/2}$ and 3d $^2D_{5/2}$ levels, and the results from collisional-radiative calculations for a few values of the electron density and temperature. It can be seen that when the POS is applied ($2.2\ \mu s \leq t \leq 2.4\ \mu s$) a density over $1 \times 10^{14}$ cm$^{-3}$ is required in order to explain the line ratio.

makes it sensitive to the density, since two collisions have to be frequent enough as not to allow the radiative decay from the 3p level to occur between the collisions.

The ratio between the level populations is shown in Fig. 6. The ratio shown represents an average over ≈80 flashboard discharges with the doping column formed at a few radial positions ($2.2\ \text{cm} \leq r \leq 4.2\ \text{cm}$) and axial positions ($-3.5\ \text{cm} \leq z \leq 3.5\ \text{cm}$). For the time at which optimal POS operation is obtained ($2.2\ \mu s \leq t \leq 2.4\ \mu s$) the ratio is almost constant, $17 \pm 1.5$. The results of the CR-code calculations for a few electron densities and temperatures are indicated by the symbols on the graph. The times at which the calculated ratios are shown are the times at which the density values are determined by the Stark broadening (Section III-A). It should be noted, however, that in Section III-A the electron density was determined assuming singly charged ions, and that the true density is smaller when the multiply-charged ions are accounted for (as discussed in Section III-C). In order to obtain the electron density and temperature self-consistently, we first obtain an estimate of the temperature using the density determined in Section III-A. The temperature is used to determine the plasma composition from absolute level populations (Section III-C). The plasma composition is in turn used to correct the electron density and so on. For $2.2\ \mu s \leq t \leq 2.4\ \mu s$ this self-consistent, iterative process yield an average temperature of $5 \pm 0.5$ eV.

A comparison of the measured and calculated level-population ratios can be used to obtain a lower bound on the electron density that is independent of the Stark broadening results. It can be seen from Fig. 6 that the calculated ratios for $n_e < 1 \times 10^{14}$ cm$^{-3}$ cannot explain the observed ratio at $2.2\ \mu s \leq t \leq 2.4\ \mu s$ (the ratio is constant for $T_e \geq 15$ eV). The lower bound obtained here is in agreement with the density obtained from the hydrogen Stark broadening measurements.

### C. Plasma Composition

The plasma composition is studied by observing the line emission from the various charge states of the elements that constitute the plasma. It is found that at the times relevant for the POS operation the plasma near the cathode is mainly composed of protons with a small fraction of neutral hydrogen and heavier ions. Farther away from the cathode and closer to the flashboard there are increasing amounts of heavier ions, mostly carbon with small amounts of oxygen, silicon, and nitrogen. Copper ions were observed to arrive at the POS region only after the time at which the POS is operated. The hydrogen, oxygen, and silicon ion, as well as a considerable amount of the carbon ions, are formed from the material that is adsorbed by the graphite coating on the flashboard and by the POS electrodes, while the copper ions originate from the flashboard electrode material.

The abundance of the various ions in the plasma at two radial positions and at the time of optimal POS operation are summarized in Table I. The atomic levels from which the density of each charge state is determined using the CR-code calculations are also indicated in the table. The CR calculations also took into account charge-exchange processes of the type $C^{Z+1} + H \rightarrow p + C^Z$ (excited). For our plasma parameters, the CIV level populations were especially found to be affected by these processes.

In Section III-A, the electron density is determined from the hydrogen Stark broadening assuming that $n_e^{\text{Stark}} = n_i$ (where $n_i$ is the ion density) i.e., singly charged ions. However, the plasma also contains multiply-charged ions, and the contribution of each ion species to the Holtsmark electric field is proportional to $n_i^{2/3} Z_i^j$, where $Z_i^j$, $n_i^j$ are the charge and density of each ion species, respectively. Therefore, the density should be corrected by: $n_e^{\text{true}} = n_e^{\text{Stark}} \cdot [\sum Z_i^j n_i^j / \sum (Z_i^j)^{3/2} n_i^j]$ [34]. It can be seen from Table I that the true electron density is 10–25% lower than that determined in Section III-A. The proton density in Table I is calculated by subtracting the measured ionic charge from the electron density: $n_p = n_e^{\text{true}} - \sum Z_i^j n_i^j$. Thus, while the electron density is largely uniform over the radial dimension (see Fig. 3), the plasma composition is observed to significantly differ across the inter-electrode gap.

### D. Comparison of Different Flashboard Configurations

We have studied the initial plasma parameters: electron density, electron temperature, injection velocity, and azimuthal uniformity, as well as the POS operation, for several flashboard configurations. It was found that as the spacing between the board with the discharge chains and the ground electrode board is increased, the injection velocity decreases, and the plasma becomes less azimuthally uniform. The azimuthal uniformity is studied by measuring the electron density from the $H_\alpha$ and $H_\beta$ Stark broadening at different azimuths.

Fig. 7 presents the electron density at $r = 2.5$ cm as a function of azimuth for two flashboard configurations. In both cases we determined the time-delay from the flashboard application to the generator firing that allows for a maximum current to be transferred to the load (at $t = 85$ ns). The density values averaged over ±100 ns at the time the POS operates are shown in Fig. 7. The azimuthal uniformity is determined from the standard deviation of the density values at the eight

TABLE I

DENSITY (IN $cm^{-3}$) OF THE PLASMA CONSTITUENTS AT TWO RADIAL POSITIONS IN THE POS INTERELECTRODE GAP. NEAR THE CATHODE (AT $r = 2$ cm) THE PLASMA IS PRIMARILY PROTONS, WHILE NEAR THE ANODE ($r = 4.5$ cm), THE MAJORITY OF THE PLASMA IS COMPOSED OF CIII-CV IONS. FOR THE INTERPRETATION OF $n_e^{Stark}$ AND $n_e^{true}$, SEE TEXT

| species | level | r=2.5 cm [$cm^{-3}$] | $Z_i n_i$ [$cm^{-3}$] | r=4 cm [$cm^{-3}$] | $Z_i n_i$ [$cm^{-3}$] |
|---|---|---|---|---|---|
| $n_e^{stark}$ | | $(2.6 \pm 0.3) \times 10^{14}$ | | $(2.4 \pm 0.3) \times 10^{14}$ | |
| CII | $4f.4s$ | $(8 \pm 2) \times 10^{11}$ | $8 \times 10^{11}$ | $(6 \pm 2) \times 10^{12}$ | $6 \times 10^{12}$ |
| CIII | $2p^2$ | $(6 \pm 1.5) \times 10^{12}$ | $1.2 \times 10^{12}$ | $(1 \pm 0.3) \times 10^{13}$ | $2 \times 10^{13}$ |
| CIV | $3p.5g.5f$ | $(6 \pm 2) \times 10^{12}$ | $1.8 \times 10^{13}$ | $(1 \pm 0.5) \times 10^{13}$ | $3 \times 10^{13}$ |
| CV | $2p$ | $(6 \pm 2) \times 10^{12}$ | $2.4 \times 10^{13}$ | $(1 \pm 0.5) \times 10^{13}$ | $4 \times 10^{13}$ |
| OII | $3p$ | $(2 \pm 0.5) \times 10^{12}$ | $2 \times 10^{12}$ | $(4 \pm 3) \times 10^{12}$ | $4 \times 10^{12}$ |
| OIII | $3p$ | $(4 \pm 1) \times 10^{11}$ | $8 \times 10^{11}$ | $(6 \pm 3) \times 10^{11}$ | $1.2 \times 10^{12}$ |
| OIV | $3d$ | $(6 \pm 2) \times 10^{11}$ | $2 \times 10^{12}$ | $(1 \pm 0.5) \times 10^{12}$ | $3 \times 10^{12}$ |
| SiII | $4d$ | $(1.5 \pm 0.5) \times 10^{11}$ | $1 \times 10^{11}$ | $(2 \pm 1) \times 10^{11}$ | $2 \times 10^{11}$ |
| SiIII | $2p^2$ | $(4.5 \pm 2) \times 10^{11}$ | $1 \times 10^{12}$ | $(2 \pm 1) \times 10^{12}$ | $4 \times 10^{12}$ |
| SiIV | $4p.5s$ | $(1 \pm 0.5) \times 10^{12}$ | $3 \times 10^{12}$ | $(2 \pm 1) \times 10^{12}$ | $6 \times 10^{12}$ |
| NII | $2p$ | $(1 \pm 0.5) \times 10^{12}$ | $1 \times 10^{12}$ | $(1 \pm 0.5) \times 10^{11}$ | $1 \times 10^{11}$ |
| NIII | $2p$ | $(1 \pm 0.5) \times 10^{12}$ | $2 \times 10^{12}$ | $(1 \pm 0.5) \times 10^{11}$ | $2 \times 10^{11}$ |
| H | $n = 3$ | $(1.5 \pm 0.2) \times 10^{13}$ | | $(1.5 \pm 0.5) \times 10^{13}$ | |
| $\sum Z_i^j n_i^j$ | | | $(6.5 \pm 3) \times 10^{13}$ | | $(11.5 \pm 5) \times 10^{13}$ |
| $n_e^{true}$ | | | $(2.1 \pm 0.3) \times 10^{14}$ | | $(1.6 \pm 0.5) \times 10^{14}$ |
| proton | - | | $(1.45 \pm 0.5) \times 10^{14}$ | | $(4.5 \pm 3) \times 10^{13}$ |

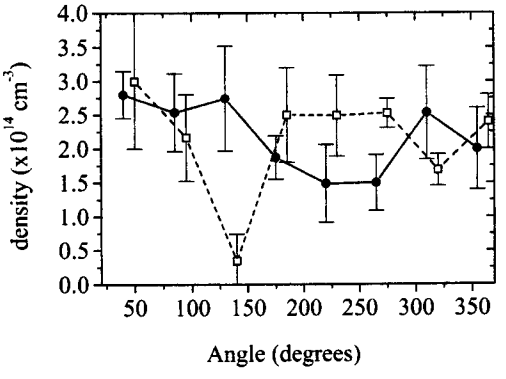


Fig. 7. Electron density as a function of azimuth for a flashboard configuration providing a load-current rise time of 15 ± 3 ns (solid squares), and for a configuration giving a load-current rise time of 27 ± 5 ns (hollow circles). The high-voltage and ground connections are at 90° and 270°. Note that measurements are taken at the same positions but are slightly shifted in the figure.

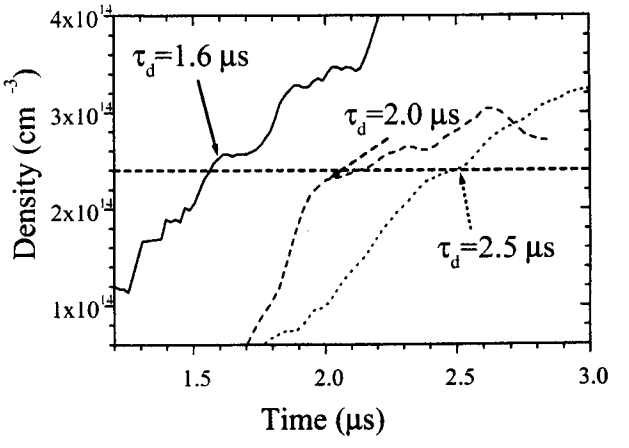


Fig. 8. Time dependent electron density determined from hydrogen line Stark broadening for three flashboard configurations having different injection velocities. The time delay for optimal POS operation for each configuration is indicated by the arrows.

azimuthal segments. For one of the configurations (hollow squares), a low density region is observed at $\theta = 135°$, and the azimuthal uniformity is ± 38%. For this configuration the POS opening time is observed to be 27 ± 5 ns. For the other configuration (solid circles), the azimuthal uniformity is ± 24%, and the POS opening time is 15 ± 3 ns. In both cases, the rise time of the load current is measured for maximal load current, occurring at $t = 85$ ns. It is clear that for a prefilled electron density, which is the more azimuthally uniform, the POS opening time is shorter.

Another important finding is that for peak current to be delivered to the load a certain electron density is required in the A–K gap, but there is no dependence on the plasma radial directed velocity. The time-dependent electron density at $r = 2.5$ cm for three flashboard configurations that produce plasma of similar axial length is shown in Fig. 8. The time delays for optimal POS operation in each configuration are indicated, showing that at this time the density is $(2.4 \pm 0.2) \times 10^{14}$ $cm^{-3}$ for all three configurations. The injection velocity of CIII is determined from the time delay of the light emission at different radii. For these three flashboard configurations the CIII velocities are $8 \times 10^6$ cm/s, $6 \times 10^6$ cm/s, and $4 \times 10^6$ cm/s. Thus, it is seen that the current conducted through the POS is similar for similar plasma density and independent of the plasma flux.

## IV. Discussion

In this section we use the experimental values of the electron density and composition to calculate the various POS conduction currents, based on the dominance of the processes mentioned in Section I. We first give quantitative predictions for the processes suggested to describe the POS operation: the widening of a cathode sheath, magnetic field penetration, and plasma pushing under the magnetic field pressure. We use cgs-Gaussian units, where $M_i$, $v_r$, $r$, and $l$ stand for the ion mass, plasma injection velocity, radial position, and plasma length, respectively. All these processes suggest that opening of the switch is achieved by magnetic insulation of the current-carrying electrons. The magnetic insulation is expected to occur at the radius where the magnetic field is strongest; i.e., next to the cathode. However, if the magnetic field propagates faster at another radius, opening is predicted to occur at this position. Since according to these models the magnetic field propagation velocity depends on the density, and since at early times the density close to the cathode is higher due to secondary plasma formation (see $r = 2.1$ cm in Fig. 3), for the estimates below we use the plasma parameters determined spectroscopically at $r = 2.5$ cm. For all calculations we use $v_r = 5 \times 10^6$ cm/s and $l = 7$ cm. The ions were assumed to be protons since at this position the plasma was shown (see Section III-A) to be proton dominated. For simplicity, we assume throughout these calculations that the generator current rises linearly in time, $\dot{I} = 2.5 \times 10^{12}$ A/s $= 7.5 \times 10^{21}$ stat A/s, which is a good approximation for our POS.

The formation of a vacuum gap that follows a sheath widening due to the plasma erosion is described by the four-phase model given in [7]. This model predicts that switch opening starts at a threshold current that is linearly proportional to the density and that is given by

$$I_{BP} = \frac{Z_i e n_i v_r 2\pi r l}{\epsilon^{1/2}} \tag{1}$$

where $\epsilon \equiv Z_i m_e / M_i$.

Several other processes that occur near the cathode have been suggested to cause current interruption. One such process is a sheath propagation along the cathode due to plasma erosion but without a vacuum gap formation. This process is described by numerical simulations [8] and recent analytical results [9]. The velocity of the sheath propagation in this modified erosion model is shown to be of the form $v_{\mathrm{ME}} = \alpha c \epsilon^{1/3}$, where $\alpha$ is of order unity and $c$ is the speed of light. It is possible that soon after the sheath reaches the load side of the plasma, opening occurs. If this is indeed the case, the current conducted before opening can be evaluated by time-integrating the velocity to find the time it takes for the sheath to reach the load side of the plasma. Such calculation yields that the maximal conduction current is

$$I_{\mathrm{ME}} = \frac{lI}{\alpha c \epsilon^{1/3}}. \tag{2}$$

For our plasma parameters the maximum conduction current in the modified erosion model $I_{\mathrm{ME}}$ is much lower than $I_{BP}$.

In addition to plasma erosion, magnetic field pressure can also widen the sheath to generate a vacuum gap. It was found [10], [11] that the propagation velocity of a sheath and the accompanying vacuum gap along the cathode due to a magnetic field pressure is $v_B = (18c^2 v_A)^{1/3}$, where $v_A \equiv 2I/[cr(4\pi n_i M_i)^{1/2}]$ is the Alfven velocity and $B = 2I/(cr)$ is the magnetic field (assuming azimuthal symmetry). Using this sheath velocity, we find the maximum conduction current to be

$$I_B = \frac{2}{3}\left[\frac{4\pi n_e M_i r^2 (l\dot{I})^6}{9c^2 Z_i}\right]^{1/8}. \tag{3}$$

Recently [11], the propagation of a sheath and a vacuum gap were studied with a more accurate form of the electric potential across the sheath. Using the asymptotic expressions derived in [11], we could show the propagation velocity to be approximated as $v_{MB} = v_B/(1+p^{4/3})$, where $p \equiv 2v_A/(3c\epsilon^{3/4})$. The maximal conduction current in this modified magnetic sheath model is then

$$I_{MB} = I_0\left[\exp\left(\frac{4l\dot{I}}{9cI_0\epsilon^{1/4}}\right) - 1\right]^{3/4} \tag{4}$$

where $I_0 \equiv (3/4)c^2 r \epsilon^{3/4}(4\pi n_i M_i)^{1/2}$.

After reviewing the predictions of the various models of sheath widening near the cathode, we turn to processes that occur in the bulk of the plasma. According to the EMHD theory [12], [13], the magnetic field penetrates into the plasma and opening occurs when the front of the magnetic field reaches the load. For a density that is almost independent of the radius (as in our experiment, see Section III-A), the penetration velocity $v_{\mathrm{EMHD}}$ is $3I/(8\pi r^2 n_e e)$ [15]. Employing this value of the penetration velocity the maximum current conducted by the POS can then be expressed as

$$I_{\mathrm{EMHD}} = \left(\frac{16\pi}{3} e n_e r^2 l \dot{I}\right)^{1/2}. \tag{5}$$

In the MHD limit, the plasma is pushed axially by the magnetic field pressure with a velocity $v_A$. For this case, the maximal conduction current is given in [15] as

$$I_{\mathrm{MHD}} = \left(\frac{12\pi M_i n_i}{Z_i}\right)^{1/4}\left(cr l \dot{I}\right)^{1/2}. \tag{6}$$

Among the processes that take place simultaneously, the dominant process in the POS operation, that process that causes the termination of the current conduction and switching to the load (opening), is the process which gives the lowest conduction current for given parameters. For example, taking the ratio of (5) and (6), we find that

$$\frac{I_{\mathrm{EMHD}}}{I_{\mathrm{MHD}}} = \left(\frac{r\omega_{pi}}{c}\right)^{1/2}\left(\frac{16\pi Z_i}{27}\right)^{1/4} \tag{7}$$

where $\omega_{pi} \equiv (4\pi n_i Z_i^2 e^2/M_i)^{1/2}$. Thus, if $r \ll c/\omega_{pi}$ (the familiar condition that the EMHD mechanism is dominant) we obtain $I_{\mathrm{EMHD}} \ll I_{\mathrm{MHD}}$ and vice versa.

The dependence of the current conducted by the POS on the prefilled plasma density, as determined in the experiment and as predicted by the theoretical models described above,

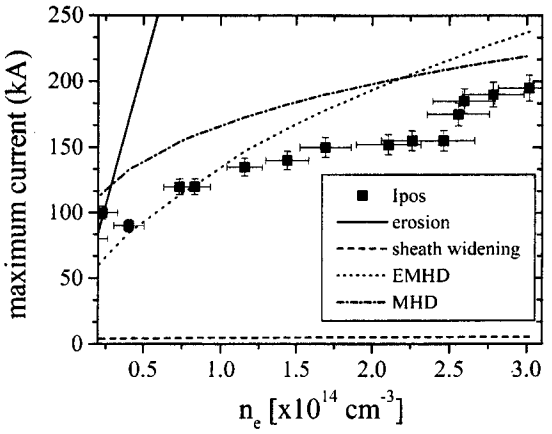


Fig. 9. Dependence of conduction current on the prefilled electron density measured in the experiment and as predicted by the four theoretical models discussed. The symbols represent the experimental data, and the solid, dashed, dotted, and dash-dotted lines are the currents predicted by the erosion model (1), the modified magnetic sheath (4), the EMHD model (5), and the MHD model (6), respectively.

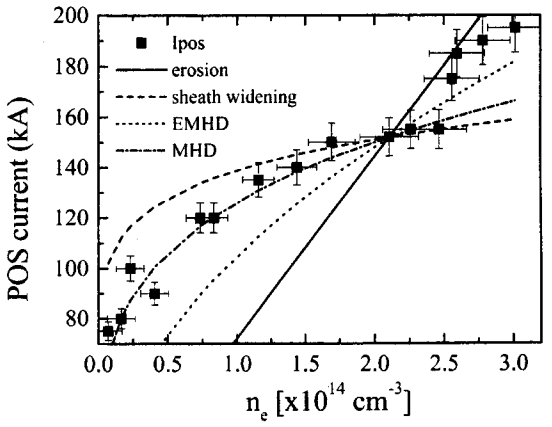


Fig. 10. Normalized dependence of the maximum POS conduction current on the prefilled electron density in the experiment and as calculated from four theoretical models. The theoretical currents have been normalized to the experimental current conducted at a density of $2 \times 10^{14}$ $cm^{-3}$. The current predicted by the MHD and EMHD models are closest to the experimental current.

is shown in Fig. 9. The theoretical curves were plotted employing (1), (4), (5), and (6). The theoretical currents given by (2) and (3) are similar to and smaller than that given by (4) and are not shown in the figure. The electron density in the experiment is varied by varying the time delay between the plasma formation and the application of the generator current pulse.

Fig. 9 clearly shows that, except for very low plasma densities, the conduction current predicted by the four-phase model is much higher than the experimental current. This suggests that (except for the low densities) erosion according to the four-phase model is not dominant in our POS. Another observation supporting this statement is that the maximum conduction current has no dependence on the plasma injection velocity (Section III-D), in disagreement with (1) which is based on the four-phase model. The conduction currents calculated by the other models involving a sheath widening near the cathode (2), (3), and (4) are much smaller than the measured conduction current. As said above, the process that occurs and allows the lowest conduction current is expected to be the process that causes the opening. Since opening is found to occur at much higher currents we conclude that sheath widening processes as described by the above models ([8]–[11]) do not occur in our experiment. The processes of sheath formation and widening and the conditions for their occurrence should be studied further both experimentally and theoretically.

Fig. 9 also shows that the values of the conduction currents calculated by the MHD and EMHD models are much closer to the experimental results than the currents predicted by sheath widening models. The current predicted by the MHD model is somewhat higher than the experimental current over the density range shown here, while the current predicted by EMHD theory is lower than the experimental one at densities below $8 \times 10^{13}$ $cm^{-3}$. At a density of $2 \times 10^{14}$ $cm^{-3}$ the predicted MHD and EMHD currents intersect, and the difference between the calculated and the experimental values is $\simeq$25%. Since the experimental values are close to both the MHD and EMHD values, we suggest that both processes of ion motion and magnetic field penetration are important during the POS operation.

It is interesting to further examine the dependence of the conduction current on the plasma parameters by using the functional density dependence predicted by (1), (4), (5), and (6). We, therefore, normalize in Fig. 10 the theoretical currents of Fig. 9 to the experimental current conducted at a density of $2 \times 10^{14}$ $cm^{-3}$. It can be seen in Fig. 10 that besides the disagreement between the values of the sheath widening models seen in Fig. 9 the functional form predicted by these models are also much different than the behavior of the experimental current. For $n_e \leq 2.5 \times 10^{14}$ $cm^{-3}$ the density dependence predicted by MHD theory is the closest to the experimentally observed dependence. At higher density, the experimental values are closer to the EMHD curve. A plausible explanation is that at the low density regime (early times with respect to the flashboard discharge) the plasma is composed mostly of protons and plasma pushing is the dominant process. At later times, the fraction of heavier ions becomes larger, and magnetic field penetration may occur before the ions can be pushed by the magnetic field.

It is important to mention again that the density determined here, based on spectroscopic observations, is almost an order of magnitude higher than previously assumed (usually based on electric-probe measurements) for ns-POS's, even for higher current generators. For example, in [26] the density in a POS of parameters similar to our POS (negative polarity, short-circuit load, $r_c = 2.5$ cm, $l = 10$ cm, $I \simeq 200$ kA) was determined using electric probes to be $\simeq 2 \times 10^{13}$ $cm^{-3}$, much lower than what we measured spectroscopically. We suggest that it is possible that the electron densities in other ns-POS's were also considerably higher than have been assumed based on probe measurements.

In Section III-D, we have shown that the POS opening time in the coaxial experiment depends on the azimuthal uniformity of the electron density. A lack of azimuthal symmetry could

result in an azimuthally nonuniform plasma pushing and magnetic field penetration, and, consequently, in a degraded POS performance. Good azimuthal uniformity can explain the better operation of a coaxial POS over the planar POS [35] (i.e., the load current rise-time is faster and the voltage multiplication is larger) and the improved planar-POS operation when two anodes are used in a tri-plate configuration [36]. Thus, improving the prefilled plasma azimuthal uniformity will lead to improvement in the operation of POS's.

## ACKNOWLEDGMENT

The authors would like to thank Yu. Ralchenko for help in the atomic physics calculation, and R. Arad and K. Tzigutin for stimulating discussions.

## REFERENCES

[1] G. Cooperstein and P. F. Ottinger, "Fast opening vacuum switches for high-power inductive energy storage," *IEEE Trans. Plasma Sci.*, vol. PS-15, pp. 629–634, Dec. 1987.

[2] C. W. Mendel Jr. and S. A. Goldstein, "Fast opening switch for use in REB diode experiments," *J. Appl. Phys.*, vol. 48, no. 3, pp. 1004–1006, Mar. 1977.

[3] R. A. Meger, R. J. Commisso, G. Cooperstein, and S. A. Goldstein, "Vacuum inductive store/pulse compression experiments on a high power accelerator using plasma opening switch," *Appl. Phys. Lett.*, vol. 42, no. 11, pp. 943–945, June 1983.

[4] J. R. Goyer, D. Kortbawi, F. K. Childers, P. S. Sincerny, b. V. Weber, P. F. Ottinger, R. J. Commisso, J. R. Thompson, and M. A. Babineau, "Plasma opening switch research for DECADE," *IEEE Trans. Plasma Sci.*, vol. 25, pp. 176–188, Apr. 1997.

[5] R. J. Commisso, J. P. Apruzese, D. C. Black, J. R. Boller, B. Moosman, D. Mosher, S. J. Stephanakis, B. V. Weber, and F. C. Young, "Results of radius scaling experiments and analysis of neon K-shell radiation data from and inductive driven Z-pinch," *IEEE Trans. Plasma Sci.*, vol. 26, pp. 1068–1085, Aug. 1998.

[6] B. V. Weber, R. J. Commisso, P. J. Goodrich, J. M. Grossmann, D. D. Hinshelwood, J. C. Kellogg, and P. F. Ottinger, "Investigation of plasma opening switch conduction and opening mechanisms," *IEEE Trans. Plasma Sci.*, vol. 19, pp. 757–765, Oct. 1991.

[7] P. F. Ottinger, S. A. Goldstein, and R. A. Meger, "Theoretical modeling of the plasma erosion opening switch for inductive storage applications," *J. Appl. Phys.*, vol. 56, no. 3, pp. 774–784, Aug. 1984.

[8] J. M. Grossmann, S. B. Swanekamp, P. F. Ottinger, R. J. Commisso, D. D. Hinshelwood, and B. V. Weber, "Gap formation processes in a high density plasma opening switch," *Phys. Plasmas*, vol. 2, no. 1, pp. 299–309, Jan. 1995.

[9] A. Fruchtman, J. M. Grossmann, S. B. Swanekamp, and P. F. Ottinger, "Sheath propagation along the cathode of a plasma opening switch," to appear in *IEEE Trans. Plasma Sci.*, vol. 27, pp. 1464–1468, Oct. 1999.

[10] C. W. Mendel, Jr., private communication, June 1998.

[11] A. Fruchtman, "A vacuum sheath propagation along the cathode," *Phys. Plasmas*, vol. 3, no. 8, pp. 3111–3115, Aug. 1996.

[12] A. Gordeev, A. S. Kingsep, and L. I. Rudakov, "Electron magnetohydrodynamics," *Phys. Rep.*, vol. 243, no. 5, pp. 215–315, July 1994.

[13] A. Fruchtman, "Penetration and expulsion of magnetic fields in plasmas due to the Hall field," *Phys. Fluids B*, vol. 3, no. 8, pp. 1908–1912, Aug. 1991.

[14] R. M. Kulsrud, P. F. Ottinger, and J. M. Grossmann, "Analysis of anomalous resistivity during the conduction phase of the plasma erosion opening switch," *Phys. Fluids*, vol. 31, no. 6, pp. 1741–1747, June 1988.

[15] B. V. Weber, R. J. Commisso, P. J. Goodrich, J. M. Grossmann, D. D. Hinshelwood, P. F. Ottinger, and S. B. Swanekamp, "Plasma opening switch conduction scaling," *Phys. Plasmas*, vol. 2, no. 10, pp. 3893–3901, Oct. 1995.

[16] W. Rix, D. Parks, J. Shannon, J. Thompson, and E. Waisman, "Operation and empirical modeling of the plasma opening switch," *IEEE Trans. Plasma Sci.*, vol. 19, pp. 400–407, Apr. 1991.

[17] J. D. Huba, J. M. Grossmann, and P. F. Ottinger, "Hall magnetohydrodynamic modeling of a long-conduction-time plasma opening switch," *Phys. Plasmas*, vol. 1, no. 10, pp. 3444–3454, Oct. 1994.

[18] R. J. Commisso, G. Cooperstein, R. A. Meger, J. M. Neri, and P. F. Ottinger, "The plasma erosion opening switch," in *Opening Switches*, A. Guenther, M. Kristiansen, and T. Martin, Eds. New York: Plenum, 1987, pp. 149–176.

[19] B. V. Weber, J. R. Boller, R. J. Commisso, P. J. Goodrich, J. M. Grossmann, D. D. Hinshelwood, J. C. Kellogg, P. F. Ottinger, and G. Cooperstein, "Microsecond conduction time POS experiments," in *Proc. 9th Int. Conf. High Power Particle Beams*, Washington, DC, 1992, vol. 1, pp. 375–384.

[20] B. V. Weber, D. D. Hinshelwood, and R. J. Commisso, "Interferometry of flashboard and cable-gun plasma opening switches on hawk," *IEEE Trans. Plasma Sci.*, vol. 25, pp. 189–195, Apr. 1997.

[21] G. G. Spanjers, E. J. Yadlowsky, R. C. Hazelton, and J. J. Moschella, "POS experiments in the MHD and EMH regimes," presented at the IEEE Int. Conf. on Plasma Sci., Madison, WI, 1995, p. 160.

[22] B. V. Weber, R. J. Commisso, R. A. Meger, J. M. Neri, W. F. Oliphant, and P. F. Ottinger, "Current distribution in a plasma opening switch," *Appl. Phys. Lett.*, vol. 45, no. 10, pp. 1043–1045, Nov. 1984.

[23] J. M. Grossmann, C. R. DeVore, and P. F. Ottinger, "Electron and ion magnetohydrodynamics effects in plasma opening switches," in *Proc. 9th Int. Conf. High Power Particle Beams*, Washington, DC, 1992, vol. 1, pp. 559–563.

[24] R. Shpitalnik, A. Weingarten, K. Gomberoff, Ya. E. Krasik, and Y. Maron, "Observations of two-dimensional magnetic field evolution in a plasma opening switch," *Phys. Plasmas*, vol. 5, no. 3, pp. 792–798, Mar. 1998.

[25] J. M. Neri, J. R. Boller, P. F. Ottinger, B. V. Weber, F. C. Young, "High-voltage, high-power operation of the plasma erosion opening switch," *Appl. Phys. Lett.*, vol. 50, no. 19, pp. 1331–1333, May 1985.

[26] B. V. Weber, R. J. Commisso, G. Cooperstein, J. M. Grossmann, D. D. Hinshelwood, D. Mosher, J. M. Neri, P. F. Ottinger, and S. J. Stephanakis, "Plasma erosion opening switch research at NRL," *IEEE Trans. Plasma Sci.*, vol. PS-15, pp. 635–648, Dec. 1987.

[27] A. B.-A. Baranga, N. Qi, and D. A. Hammer, "Flashboard plasma characterization using spectroscopy," *IEEE Trans. Plasma Sci.*, vol. 20, pp. 562–567, Oct. 1992.

[28] M. Sarfaty, Y. Maron, Ya. E. Krasik, A. Weingarten, R. Arad, R. Shpitalnik, A. Fruchtman, and S. Alexiou, "Spectroscopic investigation of the plasma behavior in a plasma opening switch," *Phys. Plasmas*, vol. 2, no. 6, pp. 2122–2137, June 1995.

[29] T. J. Renk, "Flashboards as a plasma source for plasma opening switch applications," *J. Appl. Phys.*, vol. 65, no. 7, pp. 2652–2663, Apr. 1989.

[30] H. R. Griem, *Plasma Spectroscopy*. New York: McGraw-Hill, 1964.

[31] ——, *Spectral Line Broadening in Plasmas*. New York: Academic, 1974.

[32] J. Seidel, "Spectral line shapes," in *AIP Conf. Proc.*, New York, 1990, vol. 6, no. 216.

[33] V. I. Fisher, Yu. V. Ralchenko, and Y. Maron, *Non-Maxwellian Kinetic Model*, to be published.

[34] S. Alexiou, private communication, Feb. 1998.

[35] R. J. Commisso, private communication, Nov. 1997.

[36] R. A. Riley, B. V. Weber, P. J. Goodrich, D. D. Hinshelwood, and R. J. Commisso, "Initial results of parallel-plate plasma opening switch experiments on HAWK," presented at the IEEE Int. Conf. Plasma Sci., Madison, WI, 1995, pp. 160–161.

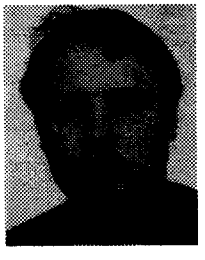

**Amit Weingarten** was born in Israel in 1965. In 1993, he received the M.Sc. degree from the Plasma Laboratory in the Physics Faculty of the Weizmann Institute of Science, Rehovot, Israel. In 1999, he received the Ph.D. degree from the Physics Faculty of the Weizmann Institute of Science

His research interests include the investigation of plasma opening switches. This research is performed mainly using spectroscopic measurements spatially resolved in 3-D of the magnetic field, the electron density, and temperature evolution.

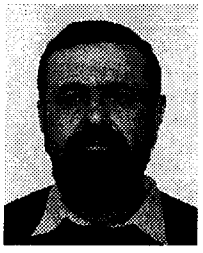

**Vladimir A. Bernshtam** was born in Kharkov, Ukraine, in 1952. He received the Ph.D. degree from Donetsk University, Ukraine, in 1983.

In 1994, he immigrated to Israel. He has been with the Plasma Laboratory at the Faculty of Physics, Weizmann Institute of Science, Israel, since 1994.

**Amnon Fruchtman**, for a photograph and biography, see p. 1468 of the October 1999 issue of this TRANSACTIONS.

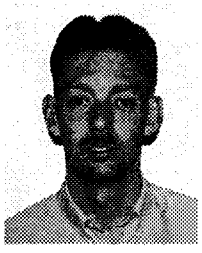

**Chris Grabowski** was born in Dayton, OH, on October 8, 1966. He received the B.S. degree in electrical engineering from Texas Tech University, Lubbock, in 1988 and the M.S. degree in electrical engineering from the University of New Mexico, Albuquerque, in 1990. He received the Ph.D. degree from the University of New Mexico, in 1997.

During 1991 and the first part of 1992, he worked as a research student in the Pulsed Power Lab at Kumamoto University, Japan. In 1997, he began postdoctoral research work in the Plasma Laboratory at the Weizmann Institute of Science, Rehovot, Israel. Currently, he has a postdoctoral position in the High Voltage Laboratory at Cornell University, Ithaca, NY, where he is working in the area of high power microwaves.

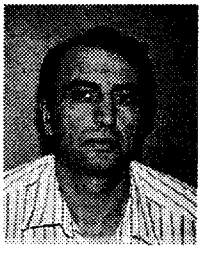

**Yakov E. Krasik** was born in Ryazan, Russia, in 1953. He received the Mc.Sc. degree in nuclear physics and the Ph.D. degree in physics and mathematics from Tomsk Polytechnical Institute, Tomsk, in 1976 and 1980, respectively. In 1991 he submitted the Dr.Sc. Thesis in physics and mathematics.

From 1980 to 1991, he was with the Nuclear Research Institute, Tomsk, Russia, as a Senior Scientist (until 1987) and as a Head of the High-Power Ion Beam Laboratory (until 1991). In 1991, he immigrated to Israel. From 1991 to 1996, he was a Senior Scientists in the Physics Department, Weizmann Institute of Science, Rehovot, Israel. He is currently a Senior Research Fellow in the Physics Department, Technion, Haifa, Israel. He has worked on high-power electron and ion beam generation, their transport, focusing and interaction with various media, plasma opening switches operated in nanosecond and microsecond time scales and active plasma cathodes based on ferroelectrics.

**Yitzhak Maron** received the physics degree from the Weizmann Institute of Science, Rehovot, Israel in 1977.

From 1980 to 1984, he worked on ion diodes at the Laboratory of Plasma Studies at Cornell University, Ithaca, NY. Since 1988, he has been a Professor of Physics and the Head of the Plasma Laboratory at the Faculty of Physics, Weizmann Institute of Science. This laboratory specializes in the use of spectroscopy in the diagnostics of pulsed power systems and in developing theoretical models requires for the data analysis and interpretation.